MATERIALS PHYSICS AND MECHANICS RESEARCH ARTICLE

Submitted: March 24, 2025 **Revised: October 15, 2025** **Accepted: March 5, 2026**

B_4C reinforced Al nanocomposite development by powder metallurgy route: revolutionizing material for the future

N. Mohanty [1], T.K. Patnaik [1], T. Dash [2]✉, S. Bajpai [3], S.K. Biswal [2]

[1] GIET University, Gunpur, Odisha, India

[2] International PranaGraf Mintech Research Centre (IGMRC), Bhubaneswar, Odisha, India

[3] CSIR-Institute of Minerals and Materials Technology, Bhubaneswar, Odisha, India

✉ tapanphy@gmail.com

ABSTRACT

An effective powder metallurgy route has been used to develop new Al/B_4C (0, 0.5, and 1 wt. %) nanocomposites. Following 4 h of optimized mechanical milling, particle size measurements verified for the pure Al, Al/B_4C (0.5 wt. %), and Al/B_4C (1 wt. %) samples as 65, 54, and 51 nm, respectively and these values are well corroborated to the crystal size measurement by XRD for the respective samples. Then the compacted (at 200 MPa) samples were sintered at an argon atmosphere at 550 °C for 3 h. Because of the homogeneous dispersion of 1 wt. % B_4C in Al, the intensity of the Al peaks is significantly reduced in the XRD pattern of Al/1 wt. % B_4C composite, which indicates the proper composite formation between Al and B_4C. It is marked that the reinforcement of B_4C enhanced the morphology of pure Al. Reinforcement of only 1 wt. % B_4C in Al was found to enhance its microhardness value from 45 to 112 VHN (about 148 % increment).

KEYWORDS

aluminium • boron carbide • XRD • microhardness

Citation: Mohanty N, Patnaik TK, Dash T, Bajpai S, Biswal SK. B_4C reinforced Al nanocomposite development by powder metallurgy route: revolutionizing material for the future. *Materials Physics and Mechanics*. 2026;54(2): 26–40. http://dx.doi.org/10.18149/MPM.5422026_3

Introduction

Aluminium (Al) is a very popular material, mainly due to its low density, ductility, and good electrical conductivity [1,2]. Still, its application is limited because of its poor hardness. Aluminium is potentially used in its alloy or composite forms. Different metals like magnesium (Mg), copper (Cu) [3], ceramics like magnesium oxide(MgO) [1], aluminium oxide (Al_2O_3), boron carbide (B_4C), silicon carbide (SiC) [3,4], and carbonaceous materials like graphene [2] and carbon nano tubes (CNT) [5] are generally added to Al to improve its various properties. Reinforcing aluminum with graphene [2] and CNT is widely used to enhance its microhardness and electrical properties. The enhancement of aluminum properties through the reinforcement of graphene/rGO and carbon nanotubes is not economically feasible. This is primarily because graphene and CNT [6] are quite expensive, which include challenges in developing aluminum-based composites using these materials. On the other hand, generally ceramic-reinforced Al matrix-based composites show good strength-to-weight ratio, corrosion, and tribological properties, enhancing their application to aviation, automobile, aerospace, marine, infrastructure, recreation, and defense [7–12].

Al with mono-, binary-, multiple-, or tri- ceramics reinforcement have been developed by different researchers [13–16]. As the number of reinforcing agents change, the behavior of composites changes with the change of kinematics and mechanism of composite formation. The process becomes challenging and difficult with the increase of number of reinforcements. Notably, among the ceramic class of carbides, boron carbide (B_4C) is the super ceramic material that shows excellent mechanical properties, low density, thermal, anti-corrosion, wear resistance, excellent impact strength, and ultimate tensile strengths, etc. [17–19].

Aluminum/boron carbide with lightweight, high hardness, and excellent thermal and chemical stability can be used for various industrial lightweight with high strength applications. Research is ongoing on B_4C-reinforced aluminium composites, but challenges include adding the right amount of B_4C, homogenous dispersion, and appropriate processing techniques. Al based composites (AMCs) can be prepared by various methods such as stir casting, powder metallurgy, squeeze casting, infiltration, spray deposition, mechanical alloying, direct metal deposition, extrusion, and hot pressing [20–23].

Each of these methods have their own Merits and demerits that are linked to specific application requirements of the composites. The powder metallurgy route is an effective method for preparing Al/B_4C composites, which involves powder composite formation, compaction, and sintering [24]. Hasan et al. [25] fabricated Al/B_4C (2.5, 5, 7.5, 10, and 12.5 wt. %) and Al/TiC (2.5, 5, 7.5, 10, and 12.5 wt. %) nanocomposites by powder metallurgy route sintered at 500 °C for 3.5 h under inert gas (argon). The micro-hardness for Al/B_4C (12.5 wt. %) nanocomposites and Al/TiC (12.5 wt. %) are 92 and 87.4 HRC, respectively, against pure Al about 40 HRC. A significant improvement in the hardness of the Al/B_4C composite was observed for the 12.5 wt. % reinforced B_4C composite. Khan et al. [23] prepared composites of AA7075 metal matrix of Al with reinforcement other ceramic like SiC, RHA (rice husk ash), and CES (carbonized eggshell) as reinforcing agents. Four samples, including AA7075, AA7075-5 wt. % SiC (MMC), AA7075-5 wt. % SiC-3 wt. % RHA (s-HMMC), and AA7075-5 wt. % SiC-3 wt. % RHA-1 wt. % CES (n-HMMC) were developed using the stir casting liquid metallurgy route, followed by the heat treatment. Stir casting of samples was carried out at 800 °C. Magnesium ribbons were added to enhance the wettability between the molten matrix and reinforcements. The cast samples underwent heat-treatment, heating at 400 °C for 3 h, quenching in a water bath, homogenization at 450 °C for 2 h, and aging at 120 °C for 24 h. The study reveals that the maximum experimental density of AA7075 was 2769 kg/m^3, with a decrease in densities with increasing reinforcements. The minimum experimental density of 2714 kg/m^3 was recorded for n-HMMC, which is about 1.18 % less than the base alloy. The reinforced composites showed higher porosity than the base alloy, with n-HMMC having the highest porosity at 3.11 %, followed by MMC, s-HMMC, and the base alloy. Scanning electron microscopy (SEM) images reveal base alloy AA7075 has coarse grains with minimal porosity, while the typical n-HMMC sample has a mixture of fine and coarse grains, with pores likely due to improper mixing, pouring issues, and trapped gases. In the work the n-HMMC alloy has the highest hardness at *HR* = 81.2 and *HBN* = 143.55, while the base alloy AA7075 has the lowest hardness at *HR* = 61.13 and *HBN* = 98.5.

Another study [26] investigates various Al-B_4C composite fabrication methods, including stir casting, powder metallurgy, melt-infiltration, and rolling. It compares their microstructural, mechanical, and physical properties. Powder metallurgy achieves uniform reinforcement particle distribution, while stir casting faces challenges like inhomogeneous distribution and low wetting behavior. Melt-infiltration is difficult to control pore size, and rolling reduces tensile strength. In our cases, heat treatment was simple and samples were sintered at relatively low temperature of 580 °C for 3 h. In our case, there is negligible reduction of density for the typical 1 wt. % B_4C reinforced Al composite in compared to base matrix of pure Al. But the microhardness value of Al was significantly increased from 45 to 112 VHN, a 148 % increase, due to the reinforcement of only 1 wt. % B_4C in Al.

Kumar et al. [27] prepared cast pure Al and Al/B_4C composites through the stir-casting method. He determined the microhardness of pure cast Al about 72 VHN. But upon addition of 6 wt. % B_4C to pure Al, it has been observed that there is an increment of about 21 VHN of composite. In [28], it is reported the effect of adding boron carbide (B_4C) reinforcement to an aluminium (Al) matrix at different volume fractions of B_4C particles, ranging from 2 to 12 %, fabricated by solid-state powder metallurgy using the hot-pressing process. The samples were processed at hot-pressing for 30 min at 620 °C, using induction heating and under uniaxial compressive stress of 60 MPa in a vacuum chamber. The hardness of the Al matrix was observed as 24 VHN. By reinforcing B_4C up to 12 vol. %, the microhardness value of the composite reached 50 VHN. No significant improvement in microhardness was observed, even when sintering was carried out at 620 °C in a vacuum chamber. Whereas the plastic deformation capacity of the Al matrix decreases as B_4C content increases. For pure Al, the material can undergo 31 % plastic deformation, which indicates a relatively high degree of ductility. However, when 12 % of B_4C is added, the plastic deformation drops significantly to 6 %. This suggests that the B_4C particles are stiffer and more brittle than Al, and their presence in the matrix inhibits the ability of the material to undergo plastic deformation. It was also marked that pure Al tends to fracture in a ductile manner, meaning it can deform plastically and absorb more energy before failure. However, with B_4C reinforced Al, the fracture becomes brittle. This transition from ductile to brittle fracture is attributed to the B_4C reinforcement. The B_4C particles are very hard and brittle, and they can act as stress concentrators within the Al matrix. When subjected to stress, these particles do not deform plastically like the Al matrix, but rather they promote crack initiation and propagation, leading to brittle fracture. In summary, while the addition of B_4C improves the hardness of the Al matrix, it also leads to a reduction in plastic deformation and a shift in fracture behavior from ductile to brittle. This makes the composite more rigid but less tough, meaning it can withstand higher stresses but is more prone to fracture under certain conditions. Hence, more additions of ceramics like B_4C are not suitable for the metallic behavior of Al.

The presented study investigates the effect of B_4C wt.% reinforcement (less or equal 1 wt. %) on the microstructural, physical and micro hardness properties of aluminium composites. Generally, B_4C more than 1 wt. % is added in pure Al to enhance its properties [17,24,25,27–29]. However, this research fills a gap in the exploration of the Al/B_4C composites synthesis by typical powder metallurgy route with sintering temperature below 600 °C. with minimum reinforcement of B_4C (preferably less than 1 wt. %) with

improved microstructural and microhardness behavior. More addition of B_4C to Al will not also be economically feasible on an industrial, commercial scale. Hence, in this work, we have made an attempt to develop pure Al and Al/B_4C (0.5 and 1 wt. %) composite materials by powder metallurgy route and evaluated their microstructural and microhardness properties for various future applications.

Materials and Methods

Aluminium (particle size ⩽ 30 μm, purity ⩾ 99 % μm, and density 2.78 g/cc) and boron carbide (particle size < 10 μm, purity 98 % and density 2.52 g/cc) powder samples were procured from Sigma-Aldrich and used as the starting materials. The typical process flowsheet adopted for preparation of Al/B_4C composites with actual photographs taken during experiments are presented in Fig. 1.

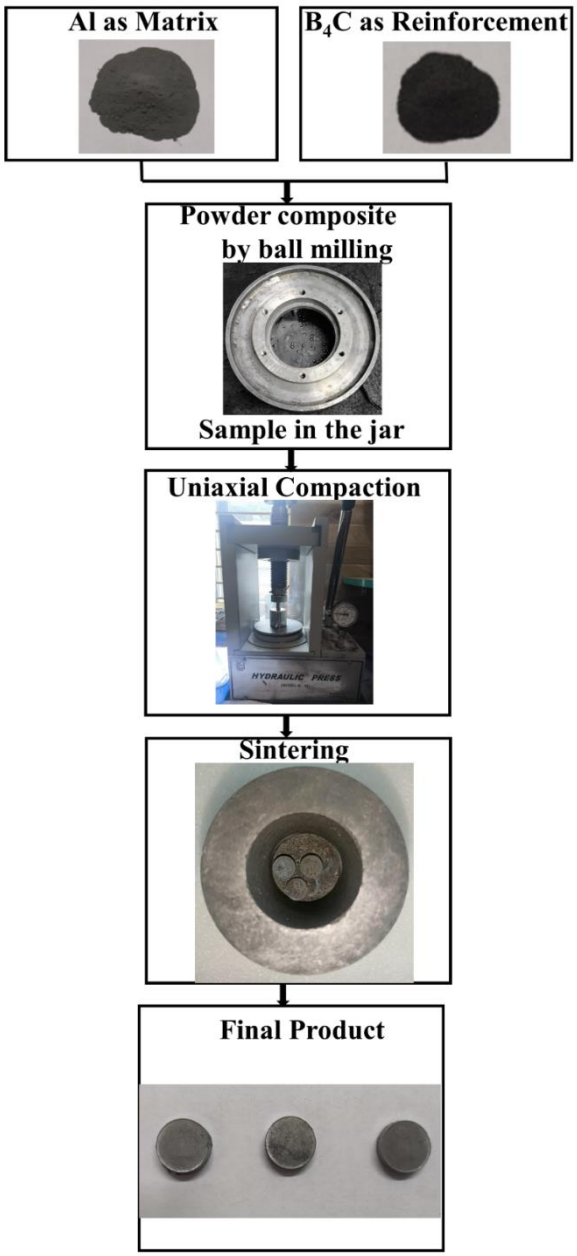

Fig. 1. The typical process flowsheet adopted for preparation of Al/B_4C composites

First, Al/B_4C (0.5 and 1 wt. %) composite powder was prepared using the mechanical planetary ball milling route. The ball mill was operated at a frequency of 30 Hz at 200 rpm (revolution per minute). Using tungsten carbide balls, the ball mill was carried in a stainless-steel jar. A charge-to-ball ratio of 1:10 was maintained during the ball milling. The milling of samples was done under an argon environment for 1–4 h. From the particle size analysis, it is observed that after 4 h of milling, the particle of power composite samples significantly reduced. The optimized powder composite samples produced after 4 h of milling were taken for cold uniaxial compaction at 200 MPa for powder samples of pure Al and Al/B4C (0.5 and 1 wt. %) composite samples added with polyvinyl alcohol (2–3 drops) as a binder. By cold compaction pellets were prepared with a diameter of 13 mm and thickness of 20 mm. Then, the pellets were air-dried. The compacted pellets were taken for sintering under an inert atmosphere (argon) in a controlled furnace. Sintering experiments were conducted at 550 °C for 180 min. After sintering over and obtaining the room temperature of the samples, they were taken out from the furnace for their properties evaluation.

The properties of the samples were evaluated using various techniques. The size distribution of mechanically ball-milled powder samples was quantified by a laser scattering particle size distribution analyzer (LA-960V2, Horiba Scientific). X-ray diffraction (XRD) (PANalytical X'Pert Pro diffractometer) was used to determine the crystalline behavior of sintered samples. Field emission scanning electron microscopy (FESEM) (model ZEISS SUPRA 55) with attached energy-dispersive X-ray spectroscopy (EDS) was employed to evaluate morphological and elemental compositions of samples after sintering. The microhardness of sintered samples was determined by taking an average of seven indentions carried out by equipment Fisher-Cripps, Australia, with diamond Berkovich indenter.

Results and Discussion

The variation of the median size (D_{50}) of mechanical ball-milled pure Al and Al/B_4C (0.5 and 1 wt. %) particles as a function of milling time (1–4 h), quantified by laser particle size analyzer is presented in Fig. 2. It has been observed that as the milling time increases from 1 to 4 h, it causes a shape decrease in particle size. From Fig. 2, it can be seen that up to 2 h of milling, there is a sharp decrease in particle size compared to the initial size of Al (particle size ⩽ 30 μm and B_4C (particle size < 10 μm). However, the rate of particle size reduction gradually decreases after 2 h of milling. In this work, we have obtained optimized particle size (D_{50}) for pure Al, Al/B_4C(0.5 wt. %), and Al/B_4C (1 wt. %) as 65, 54, and 51 nm, respectively, after 4 h mechanical milling. From Fig. 2, it can also be seen that adding B_4C particles to the Al powders resulted in a decreased size of the powder mixture. Hence, the addition of B_4C particles in Al is found to accelerate the milling process to reduce particle size. These results can be attributed to the hard ceramic behavior and finer particles of B_4C compared to Al. These results are found to be supported by other investigators regarding Al/B_4C nanocomposite powder synthesis by mechanical alloying [28].

The pure Al and Al/B_4C (0.5 and 1 wt. %) composites synthesized after 4 h of planetary ball milling were considered as the optimized nanomaterials produced in this work and then taken for cold compaction, followed by sintering experiments. The above

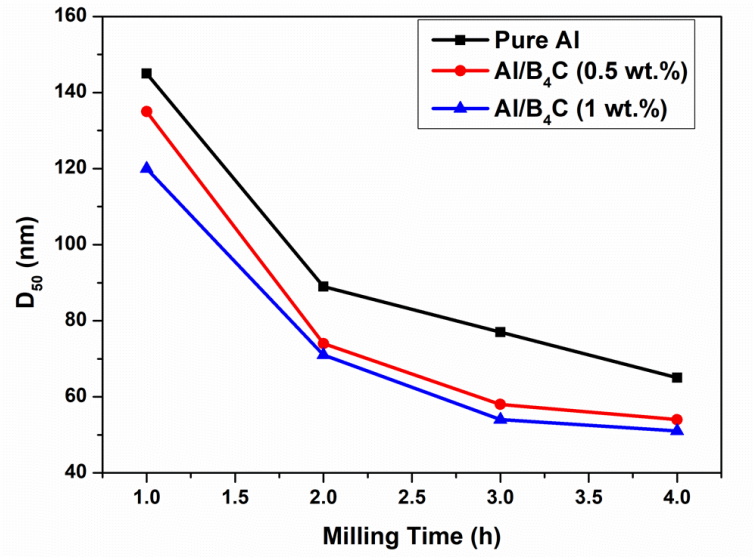

Fig. 2. The variation of the average particle size (D_{50}) of pure Al and Al/B_4C (0.5 and 1 wt. %) composites as a function of milling time

nanopowder samples added with polyvinyl alcohol (2 – 3 drops) as a binder are compacted at 200 MPa in a 13 mm die for one minute. Then, the samples were taken for sintering. In the first stage of the sintering cycle, the samples were heated from room temperature up to 550 °C with a heating rate of 5 °C per min. The samples were kept at 550 °C for 3 h in the second stage. Finally, the samples were allowed to cool up to 100 °C with a heating rate of 5 °C per min, and at last, the samples follow*ed in situ* cooling in the furnace till room temperature was achieved.

The X-ray diffraction (XRD) study of pure sintered aluminum (Al) and Al/B_4C composites with 0.5 and 1 wt. % B_4C reinforcement reveals important insights into the structural changes and crystallinity of the materials. The typical fundamental parameters obtained from XRD are presented in detail in Table 1. The diffracted peaks with their relative intensities are observable from Fig. 2. The peaks obtained in the XRD analysis are identified by comparing their Bragg's angle (2θ), d-spacing, and full width at half maximum (FWHM) values with that of inorganic crystal structure database (ICSD) of Al (Reference code: 98-006-2688) and B_4C (Reference code: 98-001-1179). In the XRD of pure sintered Al (Fig. 3(a)), distinct peaks corresponding to the (111), (002), (022), and (113) planes of aluminum are observed.

Table 1. Peak positions and corresponding FWHM and *d*-spacing values of XRD peaks of sintered pure Al and Al/B_4C composite samples

Pure Al			Al/0.5 wt.% B_4C			Al/1 wt.% B_4C			Peak assignment
Bragg's angle (2θ)	FWHM (2θ)	*d*-spacing, Å	Bragg's angle (2θ)	FWHM (2θ)	*d*-spacing, Å	Bragg's angle (2θ)	FWHM (2θ)	*d*-spacing, Å	
-	-	-	35.705210	0.048000	2.51264	35.072180	0.122803	2.55865	B_4C (104)
38.544210	0.149760	2.33562	38.518680	0.157760	2.33727	38.513900	0.185139	2.33578	Al(111)
44.806730	0.124800	2.02269	44.770120	0.192000	2.02287	44.765830	0.184205	2.02279	Al(002)
65.165870	0.149760	1.43040	65.150440	0.144000	1.43070	65.152500	0.163738	1.43106	Al(022)
78.312720	0.149760	1.21997	78.307950	0.168000	1.21991	78.299330	0.184205	1.22110	Al(113)

The XRD patterns for the Al/B_4C composites (Fig. 3(b,c)) show the presence of an additional peak at the 2θ position corresponding to the B_4C (104) plane, indicating the incorporation of B_4C particles into the Al matrix. The B_4C reinforcement does not introduce any impurity phases, confirming that the Al/B_4C composites are homogeneous. The XRD patterns of the Al/B_4C composites exhibit a shift of the aluminum peaks to lower 2θ values compared to pure Al. This could indicate lattice expansion due to the incorporation of B_4C, which is a harder material than Al. The FWHM of the peaks in Al/B_4C composites is higher than that in pure Al. The broader peaks typically suggest a reduction in crystallite size and increased lattice strain in the composite material. The FWHM is found to be the highest for the Al/B_4C (1 wt. %) composite, confirming the presence of finer grains and more internal strain. This results in a lower peak intensity for the composites. There is no significant difference in the *d*-spacing values for the corresponding peaks between pure Al and Al/B_4C composites, suggesting that the addition of B_4C does not significantly alter the crystal structure of Al at the atomic scale. The intensity of the aluminum peaks is observed to decrease with the addition of B_4C, especially in the Al/B_4C (1 wt. %) composite. This reduction in intensity is most significant for the Al (111) peak, indicating that the crystal orientation may be altered, or that there is a reduction in the size of the Al crystallites. As the B_4C content increases from 0.5 to 1 wt. % in the composites, the intensity of the B_4C (104) peak increases, confirming a higher volume fraction of B_4C in the Al matrix. This suggests that the reinforcement content has a measurable impact on the overall crystallographic structure of the composite.

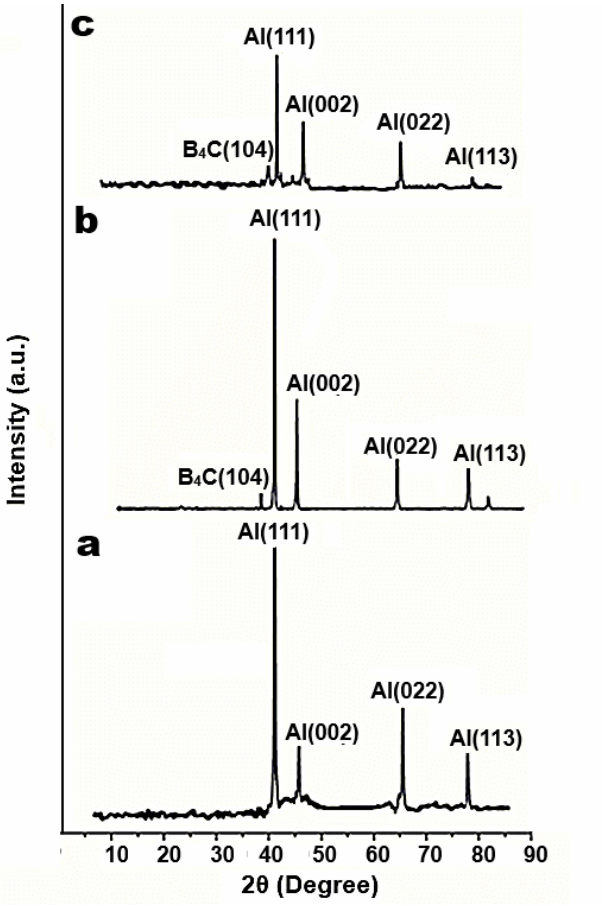

Fig. 3. XRD study of sintered samples (a) pure Al, (b) Al/B_4C (0.5 wt.%) composite, (c) Al/B_4C (1 wt.%) composite

From XRD spectra, the average crystallite size has been calculated for Al and B_4C phases considering only their highly intense peaks by applying the Scherer equation [30]:

$$\delta = \frac{0.9\lambda}{\beta cos\theta}, \quad (1)$$

where λ is a X-ray wavelength, β is FWHM (full width at half maximum) in radian for the peak observed at 2θ diffracting angle.

Pure sintered Al has a crystallite size of ~ 65.02 nm. Al/B_4C sintered composites (with 0.5 and 1 wt. % B_4C) show crystallite sizes ranging from ~ 63.88 to 64.75 nm for the Al phase and ~52.75 to 54.43 nm for the B_4C phase. The crystallite size of Al in the composites is quite similar to that of pure Al, with a slight decrease (~ 1–2 nm), suggesting that the addition of B_4C does not significantly affect the crystallite size of Al. However, the B_4C phase itself exhibits a smaller crystallite size compared to Al, which may be due to its different nature or the role of B_4C in stabilizing or refining the grains during processing. The fact that the crystallite sizes measured are consistent with the median particle sizes (D_{50}) after 4 h of milling indicates that the milling process likely contributed to refining the particles to a certain size. The lack of significant change in particle size after sintering supports the idea that milling is the dominant process for controlling particle size, rather than the sintering process itself. No significant agglomeration, grain growth, or nucleation is observed after the sintering process. This is an interesting observation, as typically, sintering can lead to particle coarsening or grain growth depending on the temperature and time. The absence of these phenomena suggests that the milling process, along with the particular sintering conditions used, was well-controlled to prevent unwanted changes in particle and grain size. It may also imply that the Al and B_4C particles were sufficiently fine and stable during milling, so no substantial changes were induced during sintering. The addition of B_4C seems to not only reduce the crystallite size of the B_4C phase but also helps to stabilize the crystallite size of the Al phase. This is likely due to the reinforcing role of B_4C particles, which may hinder excessive grain growth during the sintering process. B_4C is known for its hardness and stability, and in composites, it could act as a grain refiner, reducing the tendency of Al to grow its grains during sintering.

FESEM was used to assess the microstructure of the sintered pure Al and B_4C (0.5 and 1 wt. %) added Al composite samples (Fig. 4). There are noticeable microstructure cracks in pure sintered aluminum (Fig. 4(a)). The sample's surface morphology reveals a dip valley. After sintering, the Al/B_4C (0.5 and 1 wt. %) composite was observed to be extremely dense (Fig 4(b,c)). The microstructure shows no discernible dips or fissures. In particular, the Al/1 wt. % B_4C exhibits improved microstructure without any remarkable defects. The improvement of microhardness is greatly impacted by such superior microstructure. The study of the sintered pure Al and Al/B_4C (1 wt. %) composite phases was conducted through EDS analysis on the microstructures observed in FESEM images. The EDS analysis of sintered pure aluminium, as shown in Fig. 5(a) corresponding to the FESEM micrograph in Fig. 4(a), reveals only a peak associated with aluminium (Al). This indicates that the sintered pure Al consists solely of the aluminium phase, without any detectable impurities or additional phases. The EDS analysis of the phase 1 in the sintered Al/B_4C composite, indicated in Fig. 4(c), shows the presence of an aluminium peak (Fig. 5(b)). This confirms that phase 1 consists of aluminium, as expected in the

composite material. The EDS analysis of phase 2, marked on the FESEM image in Fig. 4(c), reveals peaks corresponding to boron (B) and carbon (C) (Fig. 5(c)). These peaks confirm the presence of the boron carbide (B_4C) phase within the composite. No peaks indicative of oxide or aluminium carbide phases were detected in the EDS analysis. The purity of the sintered samples is verified by the absence of any impurities in the EDS results, as no unexpected elements were detected, confirming the purity of the materials.

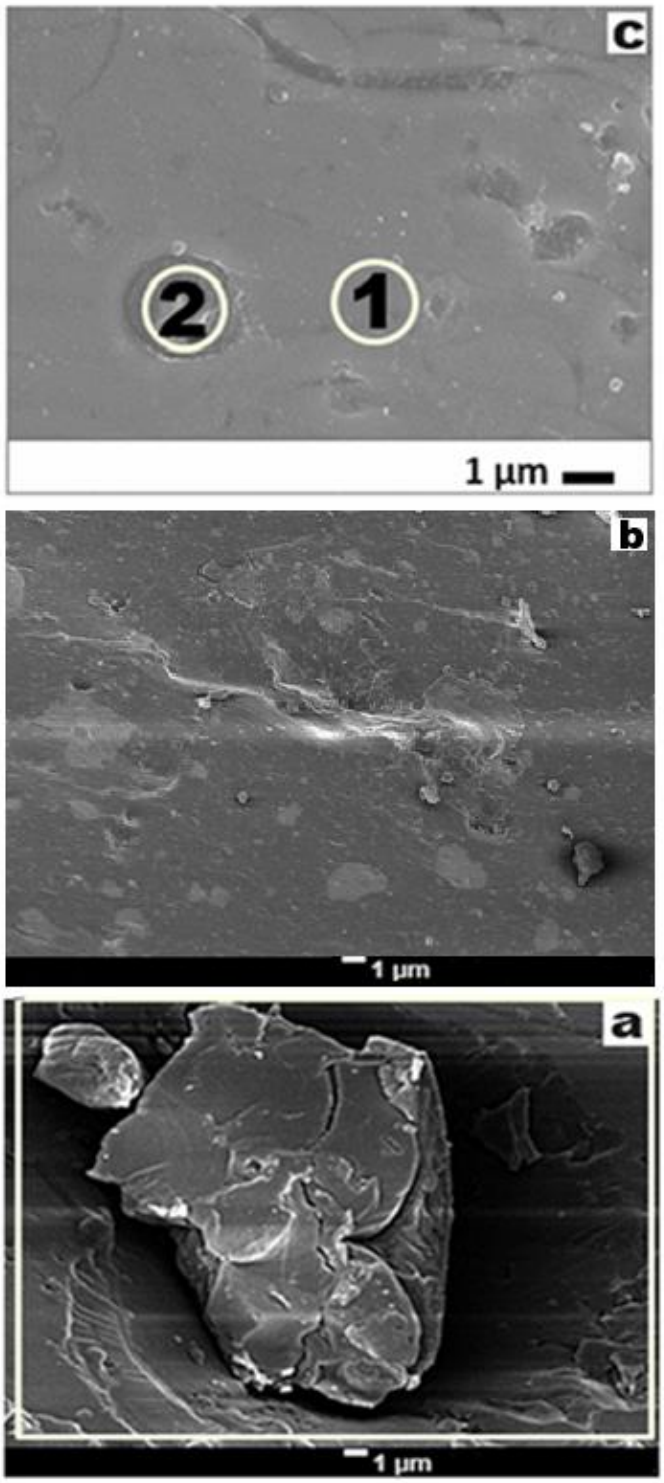

Fig. 4. FESEM analysis: (a) pure sintered Al, (b) sintered Al/B_4C (0.5 wt. %) composite sample, (c) sintered Al/B_4C (1 wt. %) composite sample

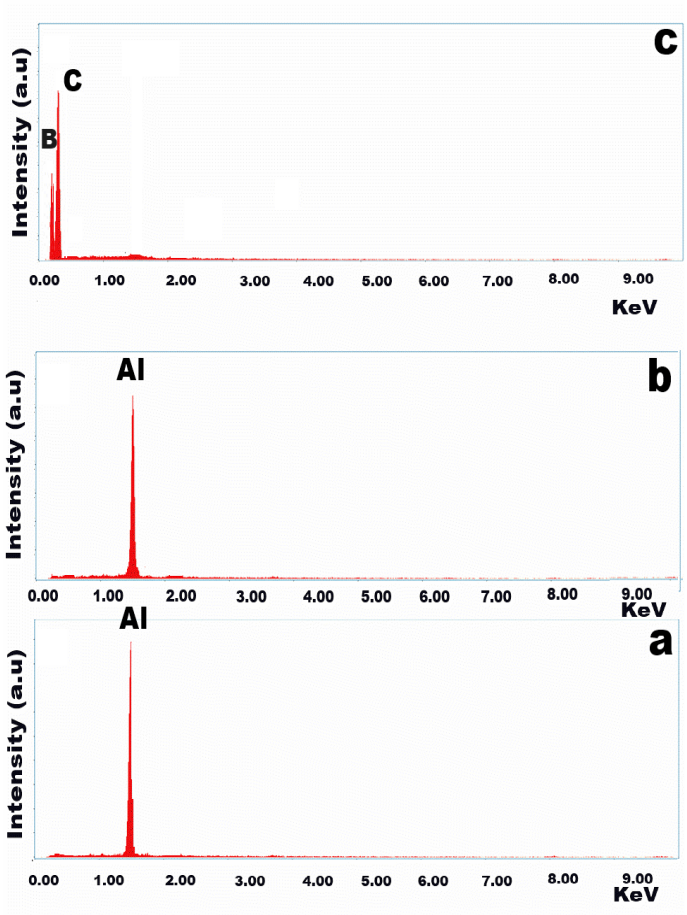

Fig. 5. (a) EDS result obtained on the total FESEM microstructure marked by the rectangular box shown in Fig. 4(a) of sintered pure Al; (b,c) EDS results obtained on the FESEM microstructure marked by phase 1 and phase 2 respectively in Fig. 4(c) of sintered Al/B_4C (1 wt. %) composite

The transmission electron microscopy (TEM) analysis result of sintered pure Al, Al/B_4C (0.5 wt. %) and Al/B_4C (1 wt. %) samples are presented in Fig. 6. Pure Al shows spheroidal kind of Al particles, which is typical for pure Al, where the particles are relatively uniform without any reinforcement. When B_4C (0.5 and 1 wt. %) reinforced in the matrix of Al, the dispersion of the B_4C particles is observed in the TEM images. The TEM results suggest that as the B_4C content increases, the particles are more evenly distributed within the Al matrix. The composite with 1 wt. % B_4C shows the relatively better dispersion, where the B_4C particles are well distributed in the Al matrix. This result could imply a stronger bond or interaction between the Al and B_4C. This analysis seems to indicate that increasing the B_4C content enhances the dispersion and potentially improves the structural integration between the phases, which might lead to improved hardness properties in the composite.

The microhardness of sintered pure Al and Al/B_4C (0.5 and 1 wt. %) composite samples were determined by calculating seven average values. The pure sintered Al exhibited a microhardness of 45 ± 5 Vickers hardness number (VHN), while the Al/B_4C (0.5 wt. %) composite demonstrated a microhardness of 75 ± 7 VHN. The microhardness of aluminum was further improved with the addition of 1 wt. % B_4C, resulting in the Al/1 wt. % B_4C composite achieving a microhardness exceeding 148 % (112 ± 8 VHN) compared to pure

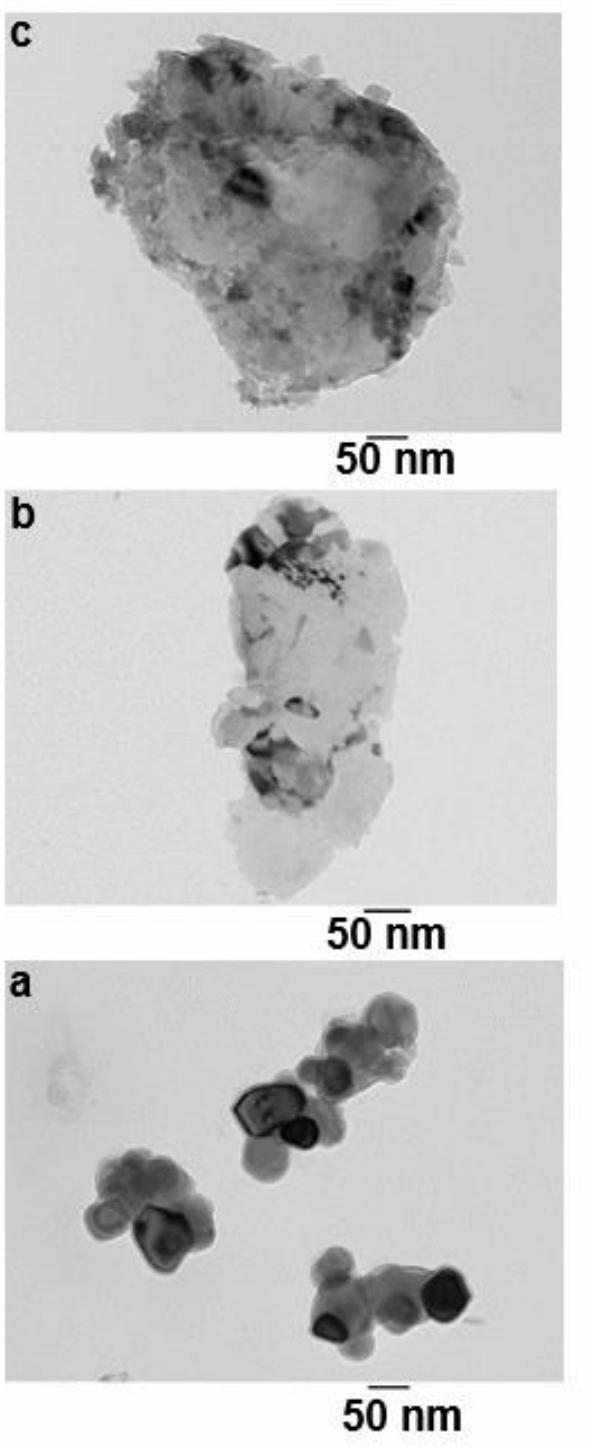

Fig. 6. TEM analysis: (a) pure sintered Al, (b) sintered Al/B_4C (0.5 wt.%) composite sample, (c) sintered Al/B_4C (1 wt.%) composite sample

aluminum. This enhancement in microhardness is attributed to the effective dispersion and presence of the harder boron carbide phase, good adhesion among the B_4C particles and Al matrix, formation of dislocations around B_4C particles due to misfit strain as well as the application of appropriate processing parameters for the production of nanocomposites.

The microhardness values of our sintered pure aluminum and aluminum/boron carbide composite samples, along with those reported in existing literature, are summarized in Table 2. In [17], a 9 wt. % addition of boron carbide to aluminum was

noted to enhance its hardness. However, our findings clearly indicate a substantial improvement in the microhardness of aluminum with only a 1 wt. % B_4C reinforcement. Nirala et al. [31] investigated boron carbide reinforcement levels ranging from 4 to 12 wt. % in aluminum, observing a maximum microhardness of approximately 77 VHN for the Al/B_4C (12 wt. %) sample with 133 % increase in microhardness from an initial value of 33 VHN for aluminum. Literature indicates that a 12 vol. % boron carbide reinforcement can elevate the microhardness of aluminum from 24 to 50 VHN, representing an increase of about 108 % [13]. Nonetheless, the reported microhardness values for aluminum tend to be lower overall. Kumar et al. [27] documented a microhardness of 72 VHN for aluminum, which increased by approximately 29 % (to 93 VHN) upon the addition of 6 wt. % boron carbide. Afrid et al. [32] reported that the microhardness of pure Al is 55.62 VHN, while that of Al with 10 wt. % reinforced B_4C composite processed by stir casting technique is 125.2 VHN. According to Gaylan et al. [33] when 5 wt. % B_4C was reinforced to the Al composite, the microhardness value was found to be 44 VHN. Upon increasing B_4C content up to 30 wt. % in the composite, the microhardness value increased to 75.5 VHN. However, when the B_4C content in the composite increased to 50 wt. %, the microhardness value decreased to 36.5 VHN. Similar kind of work was reported in [34].

Table 2. Microhardness values of pure Al and Al/B_4C composite samples

Sample	Microhardness, VHN	Method for preparation of composite	Reference
Pure Al	45.00 ± 5.00	powder metallurgy route	this work
Al/B_4C (0.5 wt. %) composite	75.00 ± 7.00	powder metallurgy route	this work
Al/B_4C (1 wt. %) composite	112.00 ± 8.00	powder metallurgy route	this work
Pure Al	72.00	stir casting technique	[27]
Al/6 wt. % B_4C	93.00	stir casting technique	[27]
Pure Al	24.00	powder metallurgy route	[13]
Al/12 vol. % B_4C	50.00	powder metallurgy route	[13]
Al/4 % B_4C	~ 33.00	stir casting technique	[31]
Al/12 % B_4C	~ 77.00	stir casting technique	[31]
Pure Al	55.62	stir casting technique	[32]
Al/10 wt. % B_4C	125.20	stir casting technique	[32]
Al/5 wt. % B_4C	44.00	powder metallurgy route	[33]
Al/30 wt. % B_4C	75.50	powder metallurgy route	[33]
Al/50 wt. % B_4C	36.50	powder metallurgy route	[33]

Generally, the literature suggests that achieving higher hardness in aluminum necessitates a considerable addition of boron carbide, which may compromise the ductility of the aluminum matrix and potentially render the process and product commercially unviable. In light of the aforementioned context, we developed a nearly uniform powder composite of Al/B_4C utilizing a specially designed planetary ball milling technique. By employing an appropriate powder metallurgy approach, we established an optimized process for the Al/B_4C composite, incorporating a minimal quantity of B_4C, specifically up to 1 wt. % in Al, to enhance the composite's properties, which was the primary aim of this study, and we successfully accomplished this goal. Our findings revealed a significant increase in hardness for the Al/B_4C composite with just 1 wt. % B_4C

reinforcement in Al, achieving a 148 % increase in microhardness compared to pure Al, all while utilizing a relatively low sintering temperature, thereby ensuring reduced energy consumption. It is widely recognized that the introduction of a ceramic phase into a metal can adversely affect its ductility. Consequently, we endeavored to create an Al/B_4C composite by incorporating a small amount (0.5 and 1 wt. %) of the ceramic phase (B_4C) to preserve the desired properties, with the expectation that the results of this research will facilitate various industrial applications of aluminum.

Conclusions

The study describes the successful synthesis of Al/B_4C composites using a powder metallurgy route. The key findings and implications are as follows:

1. The planetary ball milling process, conducted in an argon atmosphere for 1–4 h, led to a significant reduction in particle size. This nano-scale reduction is important as it can enhance the properties of the resulting composite materials. Planetary ball milling significantly reduced the particle size of the composite powders, with pure Al and Al/B_4C (0.5 and 1 wt. %) mixtures achieving nano-level particle sizes from their initial micron size. The particle sizes after 4 h of milling were measured as 65 nm for pure Al, 54 nm for Al/B_4C (0.5 wt. %), and 51 nm for Al/B_4C (1 wt. %). XRD analysis revealed no significant change in particle size post-consolidation.
2. The powder mixtures were cold compacted at 200 MPa and sintered at 550 °C for 3 h. XRD and EDS confirmed the formation of the Al/B_4C composites. The presence of B_4C, especially at 1 wt. %, reduced the intensity of the Al peaks in the XRD spectrum, suggesting strong interaction between the aluminum and boron carbide. The microstructure, as observed in FESEM images, showed a highly dense structure, critical for achieving desirable mechanical properties.
3. The hardness measurements revealed that the Al/1 wt. % B_4C composite exhibited a microhardness value of 112 ± 8 VHN, which is 148 % higher than that of pure Al. This enhancement in hardness was attributed to the reinforcement of B_4C, which notably improved the microstructure and properties of the Al matrix.
4. The addition of just 1 wt. % B_4C provided significant improvements in hardness and microstructure without any microstructural defects. This makes the Al/B_4C composite promising for various industrial applications, particularly in the aerospace sector, where material performance is critical.

Novelty and practical implications: the study's novelty lies in achieving a substantial increase in microhardness and overall structural properties with only a small amount of B_4C (1 wt. %). This approach could offer a cost-effective and commercially viable method for producing Al-based composites with significantly enhanced performance, particularly for demanding applications in sectors like automobile, aerospace, marine, etc.

CRediT authorship contribution statement

Nibedita Mohanty: investigation, data curation, writing – original draft, writing – review & editing; **Tapan Kumar Patnaik**: conceptualization, data curation, writing – review & editing, supervision; **Tapan Dash**: conceptualization, investigation, data

curation, writing – review & editing, supervision; **Shubhra Bajpai**: conceptualization; data curation; **Surendra Kumar Biswal**: conceptualization; supervision.

Conflict of interest

The authors declare that they have no conflict of interest.

References

1. Dilşad A G, Ceren B, Merve H. A review on processing, mechanical and wear properties of Al matrix composites reinforced with Al_2O_3, SiC, B_4C and MgO by powder metallurgy method. *Journal of Materials Research and Technology.* 2024;31: 1132–1150.
2. Palei BB, Dash T, Biswa SK. Graphene reinforced aluminum nanocomposites: synthesis, characterization and properties. *Journal of Materials Science.* 2022;57: 8544–8556.
3. Tamilanban T, Ravikumar T S. Influence of stirring speed on stir casting of SiC reinforced Al Mg Cu composite. *Materials Today: Proceedings.* 2021;45: 5899–5902.
4. Kumar P, Kumar D, Kaur K, Chalisgaonkar R, Singh S.S, Gupta M. Investigation of aluminum metal matrix composite fabrication processes: a comparative review. *Materials Physics and Mechanics.* 2024;52(6): 154–170.
5. Jargalsaikhan B, Bor A, Lee J, Choi H. Al/CNT nanocomposite fabrication on the different property of raw material using a planetary ball mill. *Advanced Powder Technology.* 2020;31(5): 1957–1962.
6. Kim D, Hirayama Y, Liu Z, Takagi K, Kobashi M. Fabrication of Al-CNT composite with high hardness and electrical conductivity by controlling Al_4C_3 formation. *Journal of Alloys and Compounds.* 2023;942: 169102.
7. Das D K, Mishra P C, Singh S, Thakur R K. Properties of ceramic-reinforced aluminium matrix composites - a review. *International Journal of Mechanical and Materials Engineering.* 2014;9: 6.
8. Kar A, Sharma A, Kumar S. A critical review on recent advancements in aluminium-based metal matrix composites. *Crystals.* 2024;14(5): 412.
9. Azizi Z, Rahmani K, Taheri-Behrooz F. The influence of graphene nanoplatelets addition on the electrical and mechanical properties of pure aluminum used in high-capacity conductors. *Metals.* 2022;12(11): 1883.
10. Dash T, Rout D, Palei BB. Graphene decorated aluminum nano composite with improved micro hardness and electrical conductivity. *Materials Today: Proceedings.* 2021;46: 11061–11063.
11. Kumar N, Manoj M K. Influence of B_4C on Dry Sliding Wear Behavior of B_4C/Al–Mg–Si Composites Synthesized via Powder Metallurgy Route. *Met. Mater. Int.* 2021;27: 4120–4131.
12. Sambathkumar M, Gukendran R, Mohanraj T, Karupannasamy D K, Natarajan N, Christopher D. A systematic review on the mechanical, tribological, and corrosion properties of Al 7075 metal matrix composites fabricated through stir casting process. To be published in *Advances in Materials Science and Engineering*. [Preprint] 2023. Available from: doi.org/10.1155/2023/5442809.
13. Kumar J, Singh D, Kalsi NS, Sharma S, Mia M, Singh J, Rahman MA, Khan AM, Rao KV. Investigation on the mechanical, tribological, morphological and machinability behavior of stir-casted Al/SiC/Mo reinforced MMCs. *Journal of Materials Research and Technology.* 2021;12: 930–946.
14. Aravind Senan VR, Anandakrishnan G, Rahul SR, Reghunath N, Shankar K V. An investigation on the impact of SiC/B_4C on the mechanical properties of Al-6.6Si-0.4Mg alloy. *Materials Today: Proceedings.* 2019;26: 649–653.
15. Sharma VK, Kumar V, Joshi RS, Sharma D. Experimental analysis and characterization of SiC and RE oxides reinforced Al-6063 alloy based hybrid composites. *Int J Adv Manuf Technol.* 2020;108: 1173–1187.
16. Luo J, Liu S, Paidar M, Vignesh RV, Mehrez S. Enhanced mechanical and tribological properties of AA6061/CeO2 composite fabricated by friction stir processing. *Materials Letters.* 2022;318: 132210.
17. Ravindra M R, Dilip Kumar K, Sailender M, Prasad G P, Nagaraj N, Ramulu P J. Effect of boron carbide particles addition on the mechanical and wear behavior of aluminium alloy composites. To be published in *Advances in Materials Science and Engineering.* [Preprint] 2023. Available from: doi.org/10.1155/2023/2386558.
18. Sharma D K, Sharma M, Upadhyay G. Boron Carbide (B_4C) reinforced aluminum matrix composites (AMCs). *International Journal of Innovative Technology and Exploring Engineering.* 2019;9: 2194–2203.
19. Kumar D, Kumar D, Tigga A. Processing of aluminium/boron carbide composites and functionally graded materials: A literature review. *SAE International Journal of Materials and Manufacturing.* 2022;15(2): 93–109.
20. Kumar D. Qualitative and quantitative interdependence of physical and mechanical properties of stir-

casted hybrid aluminum composites. *Materials Physics and Mechanics.* 2023;51(6): 14–23.
21. Prakash C, Singh S, Sharma S, Garg H, Singh J, Kumar H, Singh H. Fabrication of aluminium carbon nano tube silicon carbide particles based hybrid nano-composite by spark plasma sintering. *Materials Today: Proceedings.* 2020;21: 1637–1642.
22. Kumar D, Singh S. Enhancing friction and wear performance in hybrid aluminum composites through grey relational analysis. *Research on Engineering Structures and Materials.* 2024;10(3): 943-956.
23. Khan AH, Shah SAA, Umar F, Noor U, Gul RM, Giasin K, Aamir M. Investigating the microstructural and mechanical properties of novel ternary reinforced AA7075 hybrid metal matrix composite. *Materials.* 2022;15(15): 5303.
24. Zhang L, Shi J, Shen C, Zhou X, Peng S, Long X. B_4C-Al composites fabricated by the powder metallurgy process. *Applied Sciences.* 2017;7(10): 1009.
25. Hasan L K, Jiaad S M, Salman K D, Al-Maliki W A K, Alobaid F, Epple B. Wear characteristics of (Al/B_4C and Al/TiC) nanocomposites synthesized via powder metallurgy method. *Applied Sciences.* 2023;13(23): 12939.
26. Ghayebloo M, Mostaedi M T and Rad H F. A review of recent studies of fabrication of Al–B_4C composite sheets used in nuclear metal casks. *Transactions of the Indian Institute of Metals.* 2022;75: 2477–2490.
27. Kumar BNA, Ahamad A, Reddappa HN. Impact of B_4C reinforcement on tensile and hardness properties of Al-B_4C metal matrix composites. *Materials Today: Proceedings.* 2022;52: 2136–2142.
28. Brillon A, Garcia J, Riallant F, Garnier C, Joulain A, Lu Y, Silvain JF. Characterization of Al/B_4C composite materials fabricated by powder metallurgy process technique for nuclear applications. *Journal of Nuclear Materials.* 2022;565: 153724.
29. Chandrasekhar GL, Vijayakumar Y, Nagaral M, Rajesh A, Manjunath K, Kaviti RVP, Auradi V. Synthesis and tensile behavior of Al7475-nano B_4C particles reinforced composites at elevated temperatures. *Materials Physics and Mechanics.* 2024;52(3): 44–57.
30. Kawsar M, Hossain MS, Bahadur NM, Ahmed S. Synthesis of nano-crystallite hydroxyapatites in different media and a comparative study for estimation of crystallite size using Scherrer method, Halder-Wagner method size-strain plot, and Williamson-Hall model. *Heliyon.* 2024;10(3): e25347.
31. Nirala A, Soren S, Kumar N, Kaushal DR. A comprehensive review on mechanical properties of Al-B_4C stir casting fabricated composite. *Materials Today: Proceedings.* 2020;21: 1432–1435.
32. Afrid MA, Divakar MH. A Study on Effect of Stirring Speed During Fabrication of Aluminium Alloy Metal Matrix Composite. *International Research Journal of Modernization in Engineering Technology and Science.* 2022;4: 1870–1878.
33. Gaylan Y, Avar B, Panigrahi M, Aygün B, Karabulut A, Effect of the B_4C content on microstructure, microhardness, corrosion, and neutron shielding properties of Al–B_4C composites. *Ceramics International.* 2023;49(3): 5479–5488.
34. Chen H S, Wang W X, Li Y L, Zhou J, Nie H H, Wu Q C, The design, microstructure and mechanical properties of B_4C/6061Al neutron absorber composites fabricated by SPS. *Materials & Design.* 2016;94: 360–367.